

A LIMIT ON THE WARM DARK MATTER PARTICLE MASS FROM THE REDSHIFTED 21 CM ABSORPTION LINE

MOHAMMADTAHER SAFARZADEH¹, EVAN SCANNAPIECO¹, ARIF BABUL²

¹ School of Earth and Space Exploration, Arizona State University, mts@asu.edu

² Department of Physics and Astronomy, University of Victoria, Victoria, BC, V8P 5C2, Canada

ABSTRACT

The recent EDGES collaboration detection of the 21-cm absorption signal at a central frequency of $\nu = 78 \pm 1$ MHz points to the presence of a significant Lyman- α background by a redshift of $z = 18$. The timing of this signal constrains the dark matter particle mass (m_χ) in the warm dark matter (WDM) cosmological model. The small scale structure in the WDM model has a delayed formation time and therefore, requiring sufficiently strong Ly- α background due to star formation at $z = 18$, a stringent lower limit can be placed on m_χ . Our results show that the coupling the spin temperature to the gas through Ly- α pumping requires a minimum mass of $m_\chi > 4$ keV if atomic cooling halos dominate the star formation rate at $z = 18$, and $m_\chi > 3$ keV if H_2 cooling halos also form stars efficiently at this redshift. These lower limits match or exceed the most stringent limits cited to date in the literature, even in the face of the many uncertainties regarding star-formation at high redshift.

1. INTRODUCTION

Recently the EDGES collaboration (Experiment to Detect the Global Epoch of reionization Signature; [Bowman & Rogers 2010](#)) detected a global absorption signal of the redshifted 21-cm line at a central frequency of $\nu = 78 \pm 1$ MHz ($z = 17.2$), with a brightness temperature $T = -500^{+200}_{-500}$ mK and a signal-to-noise ratio of ≈ 37 ([Bowman et al. 2018](#)). This points to the indirect coupling of the spin temperature (T_S) to the gas temperature (T_K) through the Wouthuysen-Field (WF) effect ([Wouthuysen 1952](#); [Field 1957](#)) by a background of Ly- α photons at a time ≈ 180 million years after the Big Bang.

The spin temperature of HI is related to the gas (T_K), cosmic microwave background (T_γ), and Ly- α background (T_α) temperatures by

$$T_S^{-1} = \frac{T_\gamma^{-1} + x_c T_K^{-1} + x_\alpha T_\alpha^{-1}}{1 + x_\alpha + x_c}, \quad (1)$$

where x_c is the collisional coupling constant and x_α is the coupling coefficient to Ly- α photons ([Chen & Miralda Escude 2004](#); [Hirata 2006](#); [Pritchard & Furlanetto 2006](#)) given by

$$x_\alpha = \frac{8\pi\lambda_{Ly\alpha}^2\gamma T_*}{9A_{10}T_\gamma} S_\alpha J_\alpha = 1.81 \times 10^{11} \frac{J_\alpha S_\alpha}{1+z}, \quad (2)$$

where $\gamma = 50$ MHz is the half width at half-maximum of the Ly- α resonance, $T_* = h\nu_{10}/k_B = 68.2$ mK with $\nu_{10} = 1.42$ GHz, $A_{10} = 2.87 \times 10^{-15} s^{-1}$ is the spontaneous emission coefficient of the 21 cm line, J_α is the background Ly- α intensity (in units of $cm^{-2} s^{-1} Hz^{-1} sr^{-1}$), and S_α is a factor that accounts for spectral distortions, which is less than 1 when the spin and gas temperature

are similar ([Hirata 2006](#)).

As x_α increases, the spin temperature shifts from the microwave background temperature to T_α , providing information about the temperature of the high-redshift intergalactic medium. Interestingly, the best fit value of this temperature is lower than expected, potentially suggesting a subcomponent of dark matter particles with masses in the MeV range and charges a fraction of that of the electron ([Muñoz & Loeb 2018](#); [Barkana 2018](#); [Barkana et al. 2018](#)).

At the same time, warm dark matter (WMD) candidates with masses in the keV range have been proposed to account for several tensions between observations and theoretical predictions. In particular, (i) cold dark matter (CDM) cosmological simulations predict cuspy halos profiles while observations point to more core-like centers ([Bullock et al. 2001](#); [Gentile et al. 2004](#); [Kuzio de Naray et al. 2008](#); [de Blok 2010](#); [Dutton et al. 2011](#); [Rocha et al. 2013](#)); (ii) CDM simulations predict larger stellar velocity dispersions than observed in Milky Way's satellite galaxies ([Boylan-Kolchin et al. 2012](#)); and (iii) the number of subhalos predicted in the CDM simulations far exceeds the observed number of luminous Milky Way satellites ([Klypin et al. 1999](#); [Moore et al. 1999](#)).

While it remains a matter of debate whether the resolution of these tensions can be achieved by improving models of the baryonic physics in the simulations, WDM particles could also address these issues by suppressing the formation of small-scale structure. WDM particles, such as sterile neutrinos ([Dodelson & Widrow 1994](#); [Abazajian et al. 2001](#); [Shaposhnikov & Tkachev 2006](#)) and gravitinos ([Gorbunov et al. 2008](#)), remain relativistic for a longer time in the universe. This leads to non-negligible velocity dispersion which causes them to

free stream out of small scale perturbations, attenuating the matter power spectrum above a characteristic comoving wave number (Bode et al. 2001; Viel et al. 2005) of

$$k_{\text{FS}} = 15.6 \frac{h}{\text{Mpc}} \left(\frac{m_\chi}{1\text{keV}} \right)^{4/3} \left(\frac{0.12}{\Omega_{\text{DM}} h^2} \right)^{1/3}, \quad (3)$$

which leads to less pronounced cusps and fewer and smaller-mass Milky Way satellites.

Various approaches have been adopted to provide lower bounds on m_χ , which in turn place lower limits on k_{FS} . Based on the abundance of $z = 6$ galaxies in the Hubble Frontier Fields, Menci et al. (2016) arrive at $m_\chi > 2.4$ keV (2σ) and Corasaniti et al. (2017) arrive at $m_\chi > 1.5$ keV (2σ) based on the galaxy luminosity function at $z \sim 6 - 8$. The current best lower limit of $m_\chi > 3.3$ keV (2σ) is based on the high redshift Ly- α forest data (Viel et al. 2013).

The detection of the redshifted 21-cm background is also able to provide such a limit on m_χ , based on the simple fact that enough small-scale structures must collapse at high redshift to lead to a Ly- α background strong enough to couple T_S to T_α at the high end of the absorption trough, just beyond $z = 18$. The greater the suppression of small dark-matter halos, the more difficult it is for Ly- α to couple the spin and the gas temperatures by WF effect, and thus by calculating the maximum Ly- α intensity allowed as a function the rate of dark matter collapse, we are able derive a minimum allowed value for the WDM particle.

The structure of this work is as follows. In §2 we show how the high-redshift halo mass function depends on m_χ , and relate this mass function to the Ly- α background. In §3 we show how the delayed formation of halos would place lower limits on m_χ , depending on whether atomic or H₂ cooling halos dominate the star formation at $z = 18$.

2. METHOD

2.1. The Halo Mass Function

Throught this paper, we adopt the Planck 2015 cosmological parameters (Planck Collaboration et al. 2016a) where $\Omega_M = 0.308$, $\Omega_\Lambda = 0.692$, $\Omega_b = 0.048$ are total matter, vacuum, and baryonic densities, in units of the critical density ρ_c , $h = 0.678$ is the Hubble constant in units of 100 km/s, $\sigma_8 = 0.82$ is the variance of linear fluctuations on the $8 h^{-1}$ Mpc scale, $n_s = 0.968$ is the tilt of the primordial power spectrum, and $Y_{\text{He}} = 0.24$ is the primordial helium fraction. We compute the power spectrum for CDM and modify it according to the following formula to be appropriate for different WDM scenarios with different particle masses

$$P_\chi(k) = T^2(k) P_{\text{CDM}}(k). \quad (4)$$

where $P(k)$ denotes the power spectrum as a function of comoving wavenumber k . The transfer function is taken from CAMB (Lewis et al. 2000). and we adopt

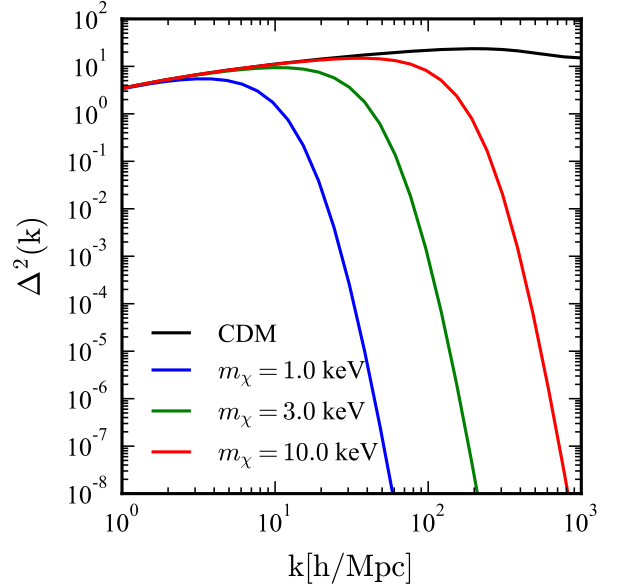


Figure 1. The normalized power spectrum $\Delta^2(k) = k^3 P(k)/(2\pi^2)$ for different cosmological models. The black line corresponds to the CDM model, while the blue, green, red and red lines correspond to the $m=1, 3$, and 10 keV WDM models respectively.

the fitting formula for $T(k)$ given by Bode et al. (2001):

$$T(k) = [1 + (\alpha k)^{2\mu}]^{-5/\mu}, \quad (5)$$

where $\mu = 1.12$ and the parameter α determines the cut off position in the power spectrum. Bode et al. (2001) related α to m_χ as

$$\alpha = \frac{0.05}{h\text{Mpc}^{-1}} \left(\frac{m_\chi}{1\text{keV}} \right)^{-1.15} \left(\frac{\Omega_{\text{WDM}}}{0.4} \right)^{0.15} \times \left(\frac{h}{0.65} \right)^{1.3} \left(\frac{g_{\text{WDM}}}{1.5} \right)^{-0.29}, \quad (6)$$

where Ω_{WDM} is the WDM contribution to the density parameter; we have set the number of degrees of freedom, $g_{\text{WDM}} = 1.5$. Figure 1 shows the power spectrum for the CDM model as compared to WDM model for $m_\chi = 1, 3$, and 10 keV.

In order to compute the halo mass function (HMF) we start with the standard Press-Schechter formalism (Press & Schechter 1974):

$$\frac{dn}{d \ln M} = \frac{\bar{\rho}}{M} f(\nu) \frac{d\nu}{d \ln M}, \quad (7)$$

where n is the number density of haloes, M the halo mass, ν the peak-height of perturbations, and $\bar{\rho}$ the average density of the universe. The first crossing distribution $f(\nu)$ is obtained with the excursion-set approach, which follows random walk trajectories counting events of first up-crossing of the collapse threshold (Bond et al. 1991). The ellipsoidal collapse model leads to a mass

dependent threshold and a first-crossing distribution of the form

$$\nu f(\nu) = A \sqrt{\frac{a\nu}{2\pi}} [1 + (a\nu)^{-p}] e^{-a\nu/2}, \quad (8)$$

with $A = 0.322$, $p = 0.3$, and $a = 0.85$ (Sheth & Tormen 2002). Here, the peak height ν is defined as $\nu \equiv \delta_{c,0}^2 \sigma_\chi(R, z)^{-2}$, with $\delta_{c,0} = 1.686$. The variance is $\sigma_\chi^2(M, z) = \sigma_\chi^2(M, 0) D(z)^2$, with

$$\sigma_\chi^2(M, 0) = \sigma_\chi^2(R, 0) = \int_0^\infty \frac{dk}{2\pi^2} k^2 P_\chi(k) w^2(kr), \quad (9)$$

where $M = 4\pi R^3 \Omega_M \rho_c / 3$, $w(kr) \equiv \frac{3j_1(kR)}{kR}$, with $j_1(x) \equiv (\sin x - x \cos x)/x^2$, and $D(z)$ is the linear growth factor

$$D(z) \equiv \frac{H(z)}{H(0)} \int_z^\infty \frac{dz'(1+z')}{H^3(z')} \left[\int_0^\infty \frac{dz'(1+z')}{H^3(z')} \right]^{-1}. \quad (10)$$

We note that we have set $a = 0.85$ in Equation 8 instead of the conventional $a = 0.75$ used in the literature. This choice is motivated by fitting the HMF redshift evolution from N-body simulations out to $z = 9$. In the top panel of Figure 2 we show the redshift evolution of the HMF compared to the Bolshoi-Planck N-body simulations out to $z = 9$ (Rodríguez-Puebla et al. 2016). Solid lines corresponds to HMFs parametrized with $a = 0.85$ and dashed lines correspond to adopting $a = 0.75$ which overshoots the amplitude of the HMF from numerical simulation towards higher redshifts. The bottom panel shows the HMF in CDM versus WDM for different values of m_χ at $z = 18$.

2.2. The Emissivity of Sources

The comoving Ly- α photon intensity at redshift z is given by (Chen & Miralda Escude 2004; Hirata 2006):

$$J_\alpha(z) = \frac{1}{4\pi} (1+z)^2 \times \int_z^{z_{\max}} \frac{c}{H(z')} \epsilon(\nu', z') dz', \quad (11)$$

where z_{\max} is determined by the condition that photons emitted at frequencies lower than the Ly- α line will not interact with the intergalactic medium

$$(1 + z_{\max}) = \frac{\nu_\beta}{\nu_\alpha} (1 + z) = \frac{32}{27} (1 + z), \quad (12)$$

where ν_β and ν_α are the Ly- β and Ly- α photon frequencies. $\epsilon(\nu', z)$ is the comoving photon emissivity (defined as the number of photons emitted per unit comoving volume, time, and frequency) at the Ly- α line from stars at redshift z :

$$\epsilon(\nu', z) = \epsilon_b(\nu_\alpha) \times \left(\frac{\nu'}{\nu_\alpha} \right)^{\alpha_s - 1} \tau_* \frac{d}{dt} \int_{M_{\min}}^\infty n(M, t) f_*(M) M dM \quad (13)$$

where $n(M, t)$ is the comoving number density of haloes per unit mass, $f_*(M)$ is the fraction of mass that is turned into stars as a function of halo mass, and

$$\epsilon_b(\nu_\alpha) = \frac{L_\alpha}{h\nu_\alpha}, \quad (14)$$

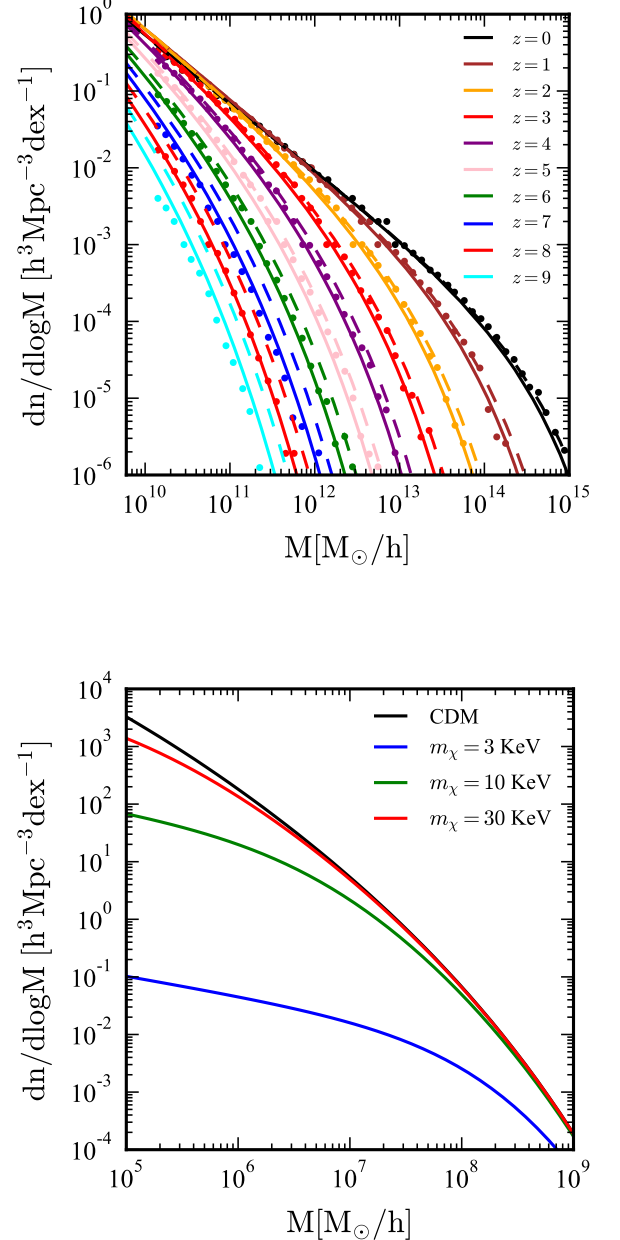


Figure 2. *Top:* The redshift evolution of our HMFs (lines) compared to the Bolshoi-Planck N-body simulations (points) out to $z = 9$ (Rodríguez-Puebla et al. 2016). Solid lines correspond to HMFs parametrized with $a = 0.85$ in Equation 8 and this is what is used in this paper. The dashed lines correspond to adopting $a = 0.75$ which is a common practice in the literature, but overshoots the amplitude of the HMF results from N-body simulation towards higher redshifts. *Bottom:* The HMF at $z = 18$. The black line corresponds to the CDM model, while the blue, green and the red lines correspond to WDM models with $m_\chi = 3, 10$, and 30 keV respectively.

where $L_\alpha = 2.7 \times 10^{21} \text{ ergs}^{-1} \text{ Hz}^{-1} M_\odot^{-1}$ for population III stars and $\tau_* = 2$ Myr is the main sequence lifetime of very massive stars [Bromm et al. \(2001\)](#), and $\alpha_s = 1.29$. [Scannapieco et al. \(2003\)](#) arrive at a slightly larger value of $L_\alpha = 3.37 \times 10^{21} \text{ ergs}^{-1} \text{ Hz}^{-1} M_\odot^{-1}$ with similar lifetime for population III stars in the mass range of 50-500 M_\odot with a top-heavy Salpeter IMF. This is by a factor of ~ 3 larger than the Ly- α yields from population III stars in the 1-500 M_\odot mass range. To be on the conservative side, we adopt the largest possible Ly- α yield of $L_\alpha = 3.37 \times 10^{21} \text{ ergs}^{-1} \text{ Hz}^{-1} M_\odot^{-1}$ in this paper.

The lower limit of the integral is set based on whether we assume atomic cooling halos dominate the SFR or the H_2 cooling halos. In the case of atomic cooling halos, the limit is $M_{\text{min}} = 4 \times 10^7 M_\odot$ at $z = 18$ where it corresponds to halos with virial temperature of $T_{\text{vir}} > 10^4 \text{ K}$.

The minimum halo mass in order for the gas to cool and condense to form stars due to both atomic and H_2 cooling based on AMR simulations ([Machacek et al. 2001](#); [Wise & Abel 2007](#)) is:

$$M_{\text{crit}} = 2.5 \times 10^5 + 1.7 \times 10^6 (F_{\text{LW}}/10^{-21})^{0.47} M_\odot, \quad (15)$$

where F_{LW} is Lyman-Werner intensity integrated over solid angle in units of $\text{ergs s}^{-1} \text{ cm}^{-2} \text{ Hz}^{-1}$. To be conservative, we consider all halos with $M > 2.5 \times 10^5 M_\odot$, ignoring the suppression of star formation due to F_{LW} .

Finally, f_* is modeled as $f_* = \epsilon_* \times f_b$ where $f_b = \Omega_m/\Omega_M$. For atomic cooling halos we adopt a conservative value of $\epsilon_* = 3\%$. This is a very generous choice as with such efficiency we are a factor of 2 above the upper bounds of the observed SFR density of $\log \dot{\rho}_* = -2.00^{+0.1}_{-0.11}$ at $z = 8$ ([Bouwens et al. 2012](#); [Madau & Dickinson 2014](#)). For H_2 cooling halos we similarly assume $\epsilon_* = 3\%$, even though this would require almost all the cold gas found in AMR simulations of early star formation to be converted into stars ([Machacek et al. 2001](#); [Wise & Abel 2007](#)).

3. RESULTS

Figure 3 shows the Ly- α coupling coefficient based on the estimated flux of Ly- α photons in WDM model as a function of m_χ for two cases: (i) only atomic cooling halos contributing to star formation at $z = 18$, and (ii) both H_2 cooling and atomic cooling halos contributing to $z = 18$ star formation.

The red (blue) regions in Figure 3 indicate the allowed range of x_α from purely atomic cooling and from atomic and H_2 cooling models respectively. Requiring coupling of gas to spin temperature to have $x_\alpha > 0.5$ through Ly- α pumping by population III stars translates into a lower bounds of $m_\chi > 3$ (4) keV if H_2 (atomic) cooling halos dominate the SFR density at $z = 18$ respectively.

The fractional difference in $\Omega_M^{0.3} \times \sigma_8$, which is a proxy for structure formation power, between the various different sets of cosmological parameters reported by Planck team ([Planck Collaboration et al. 2016b,d](#)) are $< 2\%$. We would have 4% lower structure formation

had we adopted cosmological parameters from counting

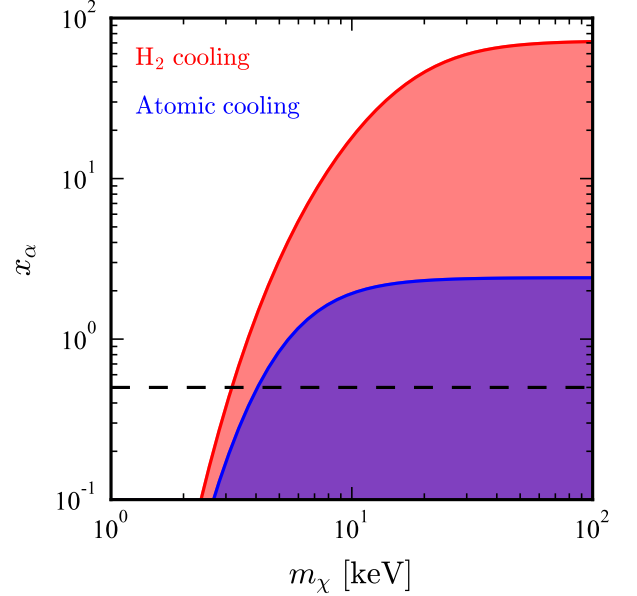


Figure 3. Ly- α coupling coefficient in the WDM model as a function of m_χ . The solid red line shows the x_α when H_2 and atomic cooling halos both contribute to the SFR density at $z = 18$ while the blue line shows the predicted x_α when only considering the atomic cooling halos. We adopt a star formation efficiency of $\epsilon = 3\%$ with minimum halo mass for star formation to be $2.5 \times 10^5 M_\odot$ for H_2 cooling halos based on numerical simulations of early structure formation ([Machacek et al. 2001](#); [Wise & Abel 2007](#)). For atomic cooling halos we adopt $\epsilon_* = 3\%$ which is a generous choice for atomic cooling halos to be on the conservative side. The red (blue) shaded regions refer to the predicted range of x_α in the two models. The black dashed line is $x_\alpha = 0.5$.

clusters ([Planck Collaboration et al. 2016c](#); [Salvati et al. 2017](#)). We would have about 3% higher structure formation had we adopted WMAP9 cosmological parameters ([Hinshaw et al. 2012](#)). We have verified that our results are not sensitive to such variations.

These lower limits match or exceed the most stringent limits achieved so far in the literature ([Viel et al. 2013](#)), even in the face of the many uncertainties regarding star-formation at high redshift. As observations and models of high-redshift galaxies continue to improve, along with detections of redshift 21 cm absorption line, comparisons of the type described here will continue to provide new insight and constraints on warm dark matter and its role in the history of structure formation.

We would like to thank Jordan Mirocha for helpful discussions. This work was supported by the National Science Foundation under grant AST17-15876, by NASA under theory grant NNX15AK82G, and by NSERC (Canada) through the Discovery Grant program.

REFERENCES

- Abazajian, K., Fuller, G. M., & Patel, M. 2001, *Physical Review D*, 64, 912
- Barkana, R. 2018, *Nature*, 555, 71
- Barkana, R., Outmezguine, N. J., Redigolo, D., & Volansky, T. 2018, eprint arXiv:1803.03091, 1803.03091
- Bode, P., Ostriker, J. P., & Turok, N. 2001, *The Astrophysical Journal*, 556, 93
- Bond, J. R., Cole, S., Efstathiou, G., & Kaiser, N. 1991, *The Astrophysical Journal*, 379, 440
- Bouwens, R. J., Illingworth, G. D., Oesch, P. A., et al. 2012, *The Astrophysical Journal*, 754, 83
- Bowman, J. D., & Rogers, A. E. E. 2010, *Nature*, 468, 796
- Bowman, J. D., Rogers, A. E. E., Monsalve, R. A., Mozdzen, T. J., & Mahesh, N. 2018, *Nature*, 555, 67
- Boylan-Kolchin, M., Bullock, J. S., & Kaplinghat, M. 2012, *Monthly Notices of the Royal Astronomical Society*, 422, 1203
- Bromm, V., Kudritzki, R. P., & Loeb, A. 2001, *The Astrophysical Journal*, 552, 464
- Bullock, J. S., Kolatt, T. S., Sigad, Y., et al. 2001, *Monthly Notices of the Royal Astronomical Society*, 321, 559
- Chen, X., & Miralda Escude, J. 2004, *The Astrophysical Journal*, 602, 1
- Corasaniti, P. S., Agarwal, S., Marsh, D. J. E., & Das, S. 2017, *Physical Review D*, 95, 638
- de Blok, W. J. G. 2010, *Advances in Astronomy*, 2010, 1
- Dodelson, S., & Widrow, L. M. 1994, *Physical Review Letters*, 72, 17
- Dutton, A. A., Conroy, C., van den Bosch, F. C., et al. 2011, *Monthly Notices of the Royal Astronomical Society*, 416, 322
- Field, G. B. 1957, *Proceedings of the IRE*, 46, 240
- Gentile, G., Salucci, P., Klein, U., Vergani, D., & Kalberla, P. 2004, *Monthly Notices of the Royal Astronomical Society*, 351, 903
- Gorbunov, D., Khmelnitsky, A., & Rubakov, V. 2008, *Journal of High Energy Physics*, 2008, 055
- Hinshaw, G., Larson, D., Komatsu, E., et al. 2012, *The Astrophysical Journal Supplement Series*, 19
- Hirata, C. M. 2006, *Monthly Notices of the Royal Astronomical Society*, 367, 259
- Klypin, A., Kravtsov, A. V., Valenzuela, O., & Prada, F. 1999, *The Astrophysical Journal*, 522, 82
- Kuzio de Naray, R., McGaugh, S. S., & de Blok, W. J. G. 2008, *The Astrophysical Journal*, 676, 920
- Lewis, A., Challinor, A., & Lasenby, A. 2000, *The Astrophysical Journal*, 538, 473
- Machacek, M. E., Bryan, G. L., & Abel, T. 2001, *The Astrophysical Journal*, 548, 509
- Madau, P., & Dickinson, M. 2014, *Annual Review of Astronomy and Astrophysics*, 52, 415
- Menci, N., Grazian, A., Castellano, M., & Sanchez, N. G. 2016, *The Astrophysical Journal*, 825, L1
- Moore, B., Ghigna, S., Governato, F., et al. 1999, *The Astrophysical Journal*, 524, L19
- Muñoz, J. B., & Loeb, A. 2018, eprint arXiv:1802.10094, 1802.10094
- Planck Collaboration, P., Ade, P. A. R., Aghanim, N., et al. 2016a, *Astronomy & Astrophysics*, 594, A13
- . 2016b, *Astronomy & Astrophysics*, 594, A13
- . 2016c, *Astronomy & Astrophysics*, 594, A24
- Planck Collaboration, P., Aghanim, N., Ashdown, M., et al. 2016d, *Astronomy & Astrophysics*, 596, A107
- Press, W. H., & Schechter, P. 1974, *The Astrophysical Journal*, 187, 425
- Pritchard, J. R., & Furlanetto, S. R. 2006, *Monthly Notices of the Royal Astronomical Society*, 367, 1057
- Rocha, M., Peter, A. H. G., Bullock, J. S., et al. 2013, *Monthly Notices of the Royal Astronomical Society*, 430, 81
- Rodriguez-Puebla, A., Behroozi, P., Primack, J., et al. 2016, *Monthly Notices of the Royal Astronomical Society*, 462, 893
- Salvati, L., Douspis, M., & Aghanim, N. 2017, eprint arXiv:1708.00697, 1708.00697
- Scannapieco, E., Schneider, R., & Ferrara, A. 2003, *The Astrophysical Journal*, 589, 35
- Shaposhnikov, M., & Tkachev, I. 2006, *Physics Letters B*, 639, 414
- Sheth, R. K., & Tormen, G. 2002, *Monthly Notices of the Royal Astronomical Society*, 329, 61
- Viel, M., Becker, G. D., Bolton, J. S., & Haehnelt, M. G. 2013, *Physical Review D*, 88, 043502
- Viel, M., Lesgourgues, J., Haehnelt, M. G., Matarrese, S., & Riotto, A. 2005, *Physical Review D*, 71, 27
- Wise, J. H., & Abel, T. 2007, *The Astrophysical Journal*, 671, 1559
- Wouthuysen, S. A. 1952, *The Astronomical Journal*, 57, 31